

Research Article

Single, double, and triple layer Prussian Blue, reduced graphene oxide, and polyaniline composite films for electrochromic applications

Hala M. Mohamed^a, Saad M. Abdel Wahab^a, Mohamed M. Abo-Aly^a, Mahmoud A. Mousa^b, Asmaa A.I. Ali^{b,*}

^a Chemistry Department, Faculty of Science, Ain-Shams University, Cairo, Egypt

^b Chemistry Department, Faculty of Science, Benha University, Benha, Egypt

ARTICLE INFO

Keywords:

Electrochromic
Prussian blue
Chronoamperometry
Chronocoulometric
Coloration efficiency

ABSTRACT

Nanoporous structures of single, binary, and ternary films from rGO, PANI, and PB materials were prepared to improve the electrochromic (EC) efficiency and electrochemical stability of electrochromic devices (ECD). Structures were prepared by electro-polymerizing aniline monomers onto coated F-doped tin oxide (FTO) glass slides with PB, rGO, or rGO/PB films, while Nickel oxide was formed by electrodeposition. The physical and optical properties of formed films were characterized by XRD, FT-IR, UV-vis, and SEM techniques. The electrochromism of the investigated electrodes was studied in 1 M LiClO₄ + propylene carbonate (LiClO₄ + PC). The properties of an electrochromic device (ECD) of glass/FTO/rGO @PANI@PB/1 M LiClO₄-PC electrolyte/NiO/FTO/glass were studied. The electrochromic properties of tested thin films were investigated using cyclic voltammograms (CV), chronoamperometry (CA), chronocoulometric (CC), and UV-Vis spectrophotometry studies. The results showed the reversible coloration and bleaching of the ECDs. The hybrid organic-inorganic materials-based electrodes improved optical modulation, switching speed, and coloration efficiency. For the different fabricated electrodes, corresponding coloring efficiencies were achieved: rGO/PANI/PB (11.3 cm²/C), rGO/PANI (4.5 cm²/C), and PANI/PB (22.8 cm²/C). Also, PANI-based electrode showed lower efficiency than PB (20.4 cm²/C vs 312 cm²/C). The promising results in this study support the use of rGO/PANI/PB electrode for smart window applications. The fabricated ECD device of (rGO/PANI/PB//NiO) achieved optical modulation (ΔT) of 41 % and switching times of 12.1 s (coloration) and 12.6 s (bleaching) at a wavelength of 625 nm. Regarding durability, the proposed ECD achieved ΔT of 38 % after 3000 cycles, i.e., 92 % of the initial device.

1. Introduction

Rapid population development and industrialization have caused serious environmental pollution and energy consumption, greatly inconveniencing human production and life [1]. Meeting increasing energy demands has become a severe challenge all around the world. The energy demand yields to global warming. Global warming occurs from carbon dioxide emission into the atmosphere due to energy production from fossil fuels [2,3]. Current development aims to develop an economical, clean energy form that is easy to control and convert and can meet the needs of different occasions [4]. Because of the limitations of non-renewable resources, improving energy utilization efficiency is an urgent problem. The fraction of the land energy reserves used in buildings for heating, cooling, ventilation, and appliances is 30–40 %. The capacity for energy saving is significant and economical in the

building domain [5,6].

Electrochromic film technology provides a new method to save energy because it controls the solar radiation and transmittance of visible light through building windows on demand [7]. When exposed to an external voltage, electrochromic materials can change color. The intercalation and deintercalation of tiny ions into and out of the material layers regulate this phenomenon [8,9]. These materials have potential uses in smart windows and gadgets because of their low power consumption and high coloration efficiency (CE) [10,11]. Electrochromic films can be deposited on the surface of conductive glass, such as fluorine-doped tin oxide (FTO) glass. Applying a different voltage range or using other electrochromic film materials will change the window's color and transmittance properties. Furthermore, the transmittance of windows can be maintained if the voltage applied is turned off. Therefore, by controlling the voltage applied to the electrochromic film,

* Corresponding author.

E-mail address: asmaa.ali@fsc.bu.edu.eg (A.A.I. Ali).

<https://doi.org/10.1016/j.optmat.2023.114589>

Received 30 July 2023; Received in revised form 2 November 2023; Accepted 6 November 2023

Available online 5 December 2023

0925-3467/© 2023 Elsevier B.V. All rights reserved.

windows can reduce the energy loss caused by the temperature difference between indoor and outdoor temperatures. Because glazed structures have lower heating and cooling costs, developing this technology may significantly reduce energy use in homes and businesses. Compared to the electrochromic window, a traditional window is responsible for the loss of approximately 30 % of the energy loss during either the cooling or heating of a building [12].

Transition metal oxides, mixed-valence materials, organic molecules, and conjugated polymers have all been produced as electrochromic materials [13–15]. In general, the EC inorganic materials are oxides separated into two classes. The first group consists of cathodic ECs, materials that change color when ions are inserted. The second category comprises materials that change color during ion extraction and are called anodic ECs [16].

Among all polymers, solution-processable conductive polymers may be used to create thin-film electrodes with customizable thickness, high conductivity, outstanding optical transparency, and superior electrochromism [17,18]. Polyaniline (PANI), particularly, has received much interest because of its electrochemical solid and thermal stabilities, adjustable characteristics, low cost, and high conductivity [19,20].

Prussian blue (PB) is a commonly utilized chemical in various applications, including sensors, electrochromic devices, and electrocatalytic electrodes [21]. Ferric hexacyanoferrate ($\text{Fe}_4[\text{Fe}(\text{CN})_6]_3$) [22] is another name for PB, which is a notable anodically electrochromic material with strong optical contrast, superior chemical stability, and quick reaction time [23]. Insoluble $\text{Fe}_4^{3+}[\text{Fe}^{2+}(\text{CN})_6]_3$ and soluble $\text{MFe}^{3+}\text{Fe}^{2+}(\text{CN})_6$, where M is an alkaline metal, are the two forms of PB. The counter electrode's composition directly influences ECD characteristics [24]. Because charge transfer and ion diffusion are directly related to surface area and gravimetric capacitance, creating high-surface-area porous electrodes can enhance pseudocapacitors' energy and power densities. Adding more porosity to the framework of Prussian blue analogs might improve their performance by creating broad pathways for easy ion mass movement in the electrode.

Nickel oxide (NiO) is cheap, abundant, and easy to make. When NiO is exposed to a voltage (V vs. RHE) = 1.35 V or higher, it undergoes a redox reaction and changes from a transparent NiO to a dark-brown NiO, which is also known as a bleached NiO or a colored NiO. The redox process of Ni(III) in alkaline conditions is well-known [25].

A five-layered sandwich-like device inside a pane of glass is used to create electrochromic smart windows. This device comprises a transparent conductor (TC) on each end, a solid electrolyte/ionic conductor (IC) in the middle, and a counter electrode between a TC and an IC on one side. The active/primary electrochromic material is located between another TC and an IC on the other side of the device. This layer controls the color change of the device. Faster ion transport might enhance the switching rate of electrochromic films because ions must be moved into and out of the film during redox reactions for electrochromic materials to retain electroneutrality [26]. As a result, a homogeneous and customizable porosity structure facilitates ion transport and the formation of redox-active films [27].

Complementary ECDs have a five-layer structure comprising anodic and cathodic coloring elements. An ionic conduction layer (electrolyte) in contact with an electrochromic (EC) layer and an ion storage (complementary) layer is sandwiched between two transparent conducting layers [28–31].

We previously reported the characterizations and electrochemical properties of nano Prussian Blue, rGO, PANI, binary, and ternary composites [32]. The electrode films were prepared using a combined spin coating and electro-polymerization methods. In this work, we studied the electrochromic of all the single, binary, and ternary hybrid films and coloration efficiencies. The triple-layer PB/rGO/PANI film demonstrates great potential for electrochromic applications. Moreover, new ECD windows with glass/FTO/rGO/PANI/PB/LiClO₄-polycarbonate/NiO/FTO/glass configuration were assembled. XRD, FTIR, and SEM-EDX will characterize the electrochromic films. Utilization spectro-electrochemical

techniques, the optical properties of the films (transmittance) will be defined. It will then be decided which coloring efficiency to use.

2. Experimental

2.1. Materials and synthesis of the electrochromic thin films

All the chemicals, except aniline, were of analytical purity and could be used without additional purification. The aniline was distilled at low pressure before use. Except for reduced graphene oxide, all samples were electrically synthesized. The working electrodes for the electrochromic were prepared according to the following methods:

- (1) A reduced graphene oxide (rGO) electrode was prepared using a modified Hummers method [33].
- (2) The cyclic voltammetric approach was utilized to develop a polyaniline film onto a glass substrate of fluorine-doped tin oxide (FTO) by utilizing a 0.5 M aniline monomer precursor in a 0.5 M aqueous solution of H₂SO₄. With a scan rate of 50 mV/s, five cycles of back-and-forth scanning from 0 to +1.2 V vs. SCE were used to carry out the electrochemical polymerization process [34].
- (3) Using a deposition solution consisting of 100 mL distilled water, 0.7455 g KCl (1 M), 3.29 g K₃[Fe(CN)₆] (1 M), and 2.70 g FeCl₃·6H₂O (1 M), Prussian Blue Film was installed on an FTO glass substrate using chronoamperometry for 10 min at potential −0.5V.
- (4) A PANI@PB composite electrode was created by deposition of PB on the surface of a PANI film using chronoamperometry at −0.5V for 10 min using a deposition solution containing 100 mL distilled water, 0.7455 g KCl (1 M), 3.29 g K₃[Fe(C.N.)₆] (1 M), and 2.70 g FeCl₃·6H₂O (1 M).
- (5) A rGO@PANI composite electrode was created by spin coating rGO on FTO glass. PANI was then deposited on rGO using chronoamperometry to polymerize aniline at potential +0.8V for 5 min from a deposition solution containing 50 mL of 0.5 M H₂SO₄ aqueous solution containing 0.5 M aniline.
- (6) The rGO@PB composite electrode was made by deposition of PB on the rGO/FTO surface by chronoamperometry at potential −0.5V for 10 min using a deposition solution of 100 mL distilled water, 0.7455 g KCl (1 M), 3.29 g K₃[Fe(C.N.)₆] (1 M), and 2.70 g FeCl₃·6H₂O (1 M).
- (7) A rGO@PANI@PB composite electrode was made by electro-polymerized aniline on the rGO/FTO surface using chronoamperometry at potential 0.8V for 5 min from a deposition solution containing 50 mL of 0.5 M H₂SO₄ aqueous solution containing 0.5 M aniline. Finally, the PB electrodeposited of the surface of PANI/rGO/FTO by chronoamperometry at potential −0.5 V for 10 min using a deposition solution of 100 mL distilled water, 0.7455 g KCl (1 M), 3.29 g K₃[Fe(C.N.)₆] (1 M), and 2.70 g FeCl₃·6H₂O (1 M).
- (8) Using a chronoamperometry approach set at −0.5 V for 10 min, NiO electrode was created by electrodeposition on cleaned FTO glass from a solution containing 50 mL of 0.2 M Ni(NO₃)₂·6H₂O. To obtain the NiO coating, the glass slide was air-dried for a day and then annealed for an hour at 300 °C in an oven in air environment.

All the organized samples were left to dry in the air overnight before performing the measurements.

2.2. Characterization tools

Scanning electron micrographs (SEM) were obtained using SEM (JEOL JSM-6460, Tokyo, Japan). XRD analyses were performed on Bruker D8 Advance diffractometer with CuK α radiation (λ : 1.54 Å). The

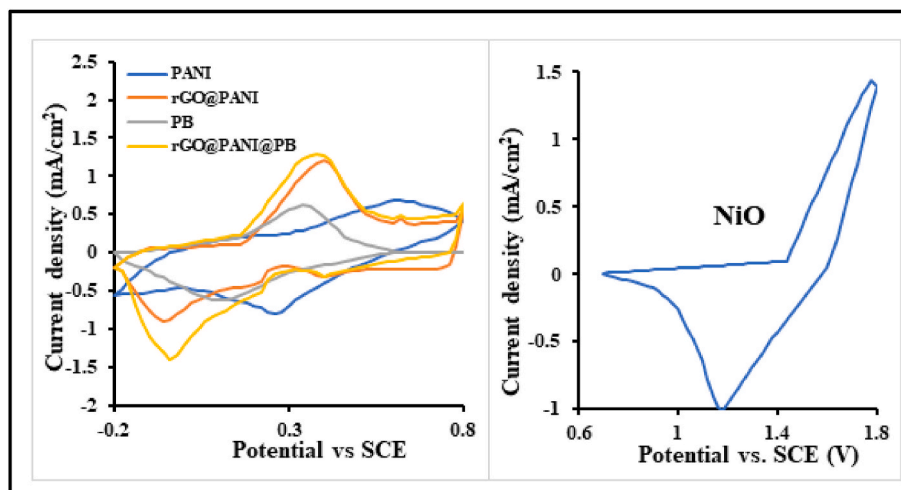


Fig. 1. Cyclic voltammogram in 1 M LiClO₄/propylene carbonate solution at 50 mV/s for (a) PB, PANI, rGO@PANI, rGO@PANI@PB thin films and (b) NiO.

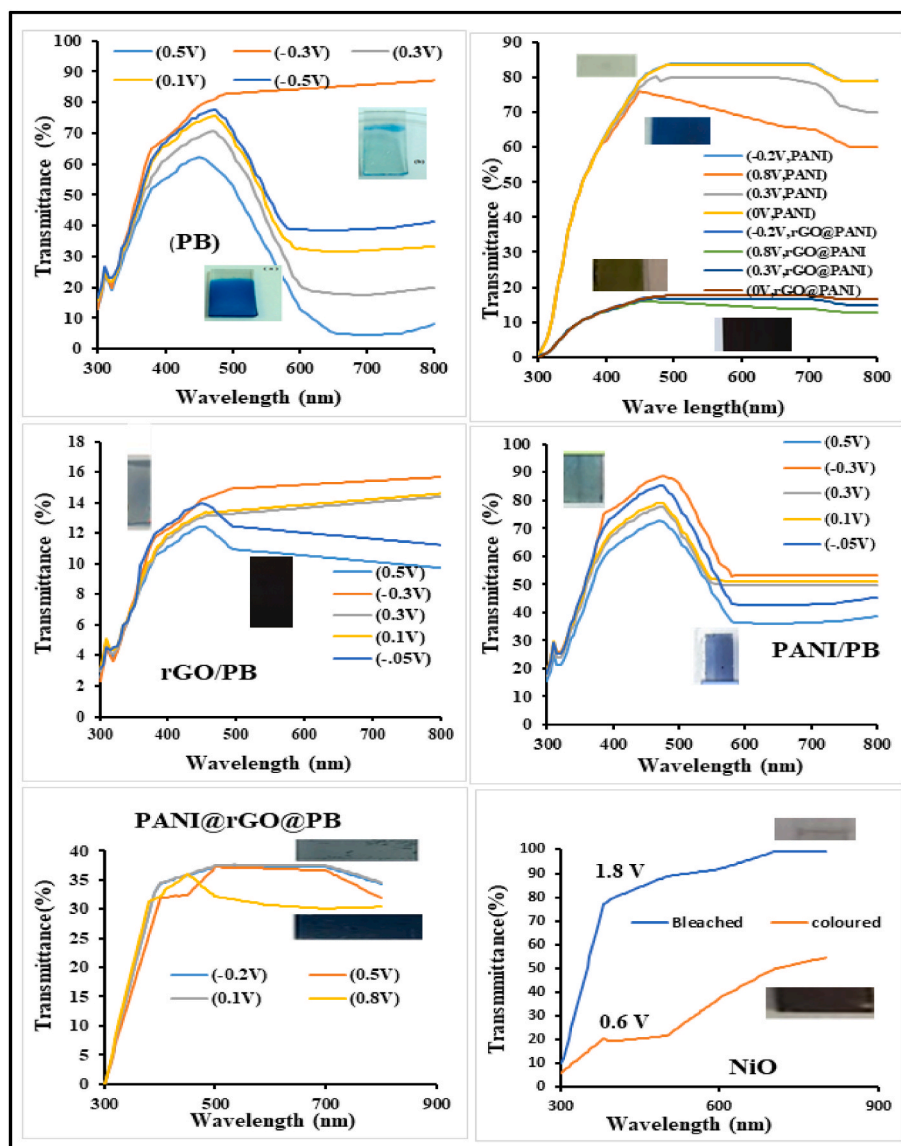


Fig. 2. In-situ UV-vis transmittance spectra of P.B., PANI, rGO, rGO@PANI, PANI@PB, rGO@PANI@PB and NiO thin films in oxidation and reduced states.

on the FTO substrate at a potential range of 0.6–1.8V/SCE show a color change from colorless (bleached) to dark brown (colored), which is attributed to the Ni^{2+} to Ni^{3+} redox process, as shown in Eq. (2).

The coloration-switching responses are crucial for evaluating electrochromic performance for energy usage and coloration-switching. The kinetic switching analysis of the investigated thin films was performed using the chronocoulometric (CC) technique to look at how the charge density of Li^+ ions changes during intercalation and deintercalation. The coloration properties of all the investigated films were reviewed by applying potential steps depending on the oxidation and reduction potential of the studied film with a pulse width of 20 s. The acquired results are represented in Figs. 3 and 4. From this, the kinetic switching values were evaluated, and the reversibility of the coloration and bleaching, which is related to the change of Li-concentration in the electrode, was calculated using Eq. 3 [36–38]:

$$\text{Reversibility}(\%) = \frac{Q_{\text{out}}}{Q_{\text{in}}} \quad (3)$$

Q_{in} and Q_{out} are the amounts of charge intercalated and deintercalated in the electrode at the electrochromic thin film's reduction and oxidation reactions.

Table 2 shows the transmittance modulations and the transmittance

difference between the bleached and colored states of electrochromic materials. Reduced transmittance modulations of rGO-containing films indicate the block effect of the injected rGO even further.

Coloration efficiency (CE) is essential for electrochromic materials in practical applications. It is defined as the change in optical density (OD) per unit charge (Q) introduced into (or withdrawn) from electrochromic films, i.e., the amount of energy required to change the color. Equations (4) and (5) are used to compute the CE [39]:

$$\text{CE} = \frac{\Delta OD(\lambda)}{Q_{\text{in}}} \quad (4)$$

$$\Delta OD(\lambda) = \log \frac{T_{\text{bleached}}}{T_{\text{colored}}} \quad (5)$$

where ΔOD is the change in the optical density, λ is the dominant wavelength for the material, Q_{out} is the charge density (injected/ejected charges per unit electrode area), T_{bleached} refers to the transmittance of the film in the bleached state, and T_{colored} refers to the varying transmittance of the film during the coloring process. The obtained data are recorded in Table 2. The thin films' stability, persistency, and switching response are also evaluated from optical transmittance measurements.

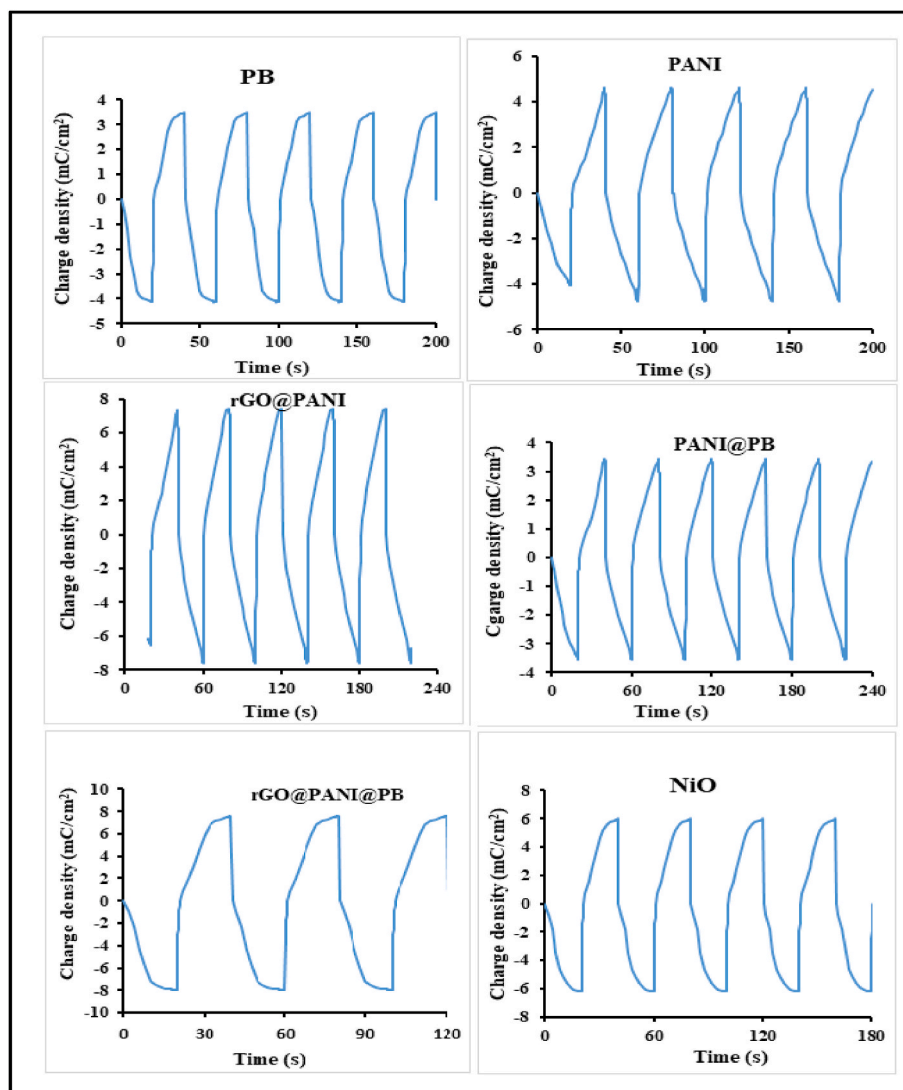


Fig. 3. The time response of the charge density during bleaching and coloring cycling during 20 s intervals for (1) PB at 700 nm with an applied voltage between 0.5 and -0.2 V vs. SCE (2) for PANI, rGO@PANI, and rGO@PANI@P.B. at 660 nm with an applied voltage between 0.8 and -0.2 V vs. SCE (3) for NiO at 500 nm during cycling of bleaching and coloring with an applied potential switched between 0.6 V and 1.8 V vs. SCE.

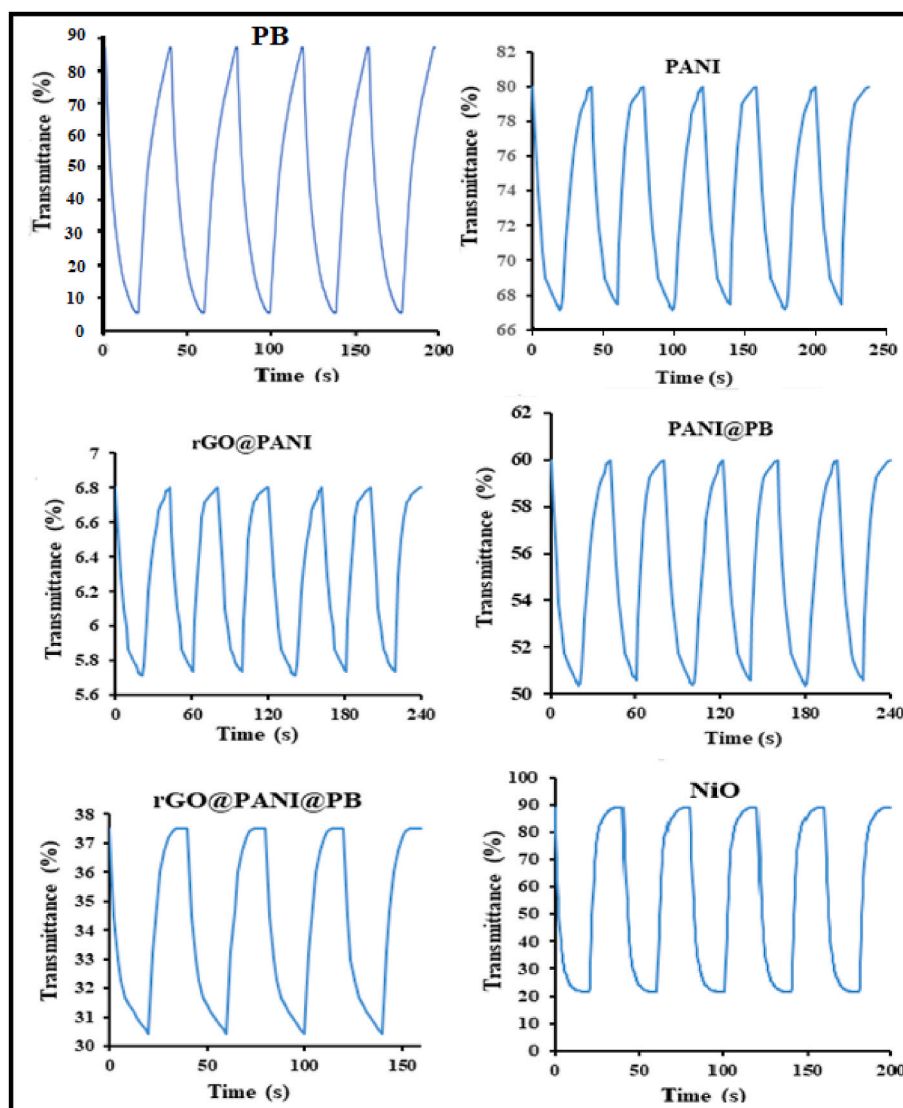


Fig. 4. The time response of the optical transmittance during bleaching and coloring cycling during 20 s intervals for (1) PB at 700 nm with an applied voltage between 0.5 and -0.2 V vs. SCE (2) for PANI, rGO@PANI, and rGO@PANI@PB at 660 nm with an applied voltage between 0.8 and -0.2 V vs. SCE (3) for NiO at 500 nm during cycling of bleaching and coloring with an applied potential switched between 0.6 V and 1.8 V vs. SCE.

Table 2

Electrochromic data of investigated thin film samples.

Sample	T (λ), nm	Q_{in}	Q_{out}	Reversibility %	Transmittance T_b	T_c	ΔT , %	Color/Bleach time (s) t_c	t_b	ΔOD	CE, cm^2/C
PB	700	4.10	3.60	87.8	86	4.5	81.5	13.1	12.1	1.28	312
PANI	650	4.90	4.60	93.9	83.7	66.5	17.2	15.1	16.2	0.10	20.4
rGO@PANI	650	5.50	5.20	94.5	16.72	17.72	1.0	16.1	17.2	0.025	4.5
PANI@PB	650	3.52	3.45	98.0	60	50.6	9.4	17.0	18.0	0.08	22.8
rGO@PANI@PB	600	7.95	7.65	96.2	37.5	30.3	7.2	5.5	5.7	0.09	11.3
NiO	500	6.20	6.00	96.7	88.8	21.6	67.2	5.7	6.2	0.61	98.3

The electrochromic switching time was calculated at 90 % of the change in optical transmittance and current density. Response time for coloration (t_c)/bleaching (t_b) is the time required for the cathodic/anodic current to reach a steady state level after the application of the respective voltage [40]. The optical density versus bias potential of electrochromic/FTO glass after 10^3 cycles in 1 M LiClO₄/PC was analyzed to evaluate the aging process. With the help of the Alpha step profiler, the thickness of the electrode was examined after 10^3 cycles. All the above-mentioned electrochromic data are recorded in Table 2. From which it can be seen that (1) A reduction in the transmittance

modulations between the bleached and colored states of PANI composite films compared to that of PANI, referring to the block effect of the introduced rGO. (2) The reversibility of the electrochromic thin films is high, especially NiO/FTO thin film (96.7) referring to their high potential for use in smart windows and display devices. (3) The CE values follow the order:

PB > NiO > PANI > rGO@PANI@PB > rGO@PANI

The drop in CE for the PANI-based nanocomposite films indicates a

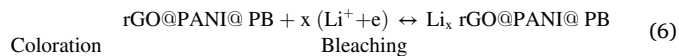
loss in color-changing response ability because high injected charges result in a more significant optical density change than the composite PANI film. (4) Switching response follows the order:

$$rGO@PANI > PANI > PB > NiO > rGO@PANI@PB$$

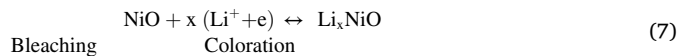
The response time of $rGO@PANI@PB$ is faster when compared with Prussian blue. This faster-switching response represents its better performance in electrochromic devices. **The functional improvements may be due to the larger surface area and pore size of mesoporous $rGO@PANI@PB$ and facilitated charge transport.** Moreover, the voids between the grains can provide important diffusion channels for ions and electrolyte molecules to migrate throughout the film [41]. The higher Li^+ diffusion coefficient in the film and shorter switching time are due to the ordered structure and high dispersion of $rGO@PANI@PB$, which results in lower ion diffusion resistance between the active component and the electrolyte. The aging value of thin electrochromic/FTO glasses after ending 3000 cycles showed values of 15, 12, 8, 5, and 3 % for PB, PANI, $rGO@PANI$, NiO, and $rGO@PANI@PB$, respectively. This demonstrates that PANI and rGO attached to PB particles significantly strengthen the structure of the $rGO@PANI@PB$ film. Thus, devices with $rGO@PANI@PB$ nano-heterojunctions would possess a more extensive ECD lifetime.

3.2.2. Electrochromic of FTO/NiO/LiClO₄/PANI@rGO@PB device (ECD)

According to the electrochromic data obtained, we designed an electrochromic device (ECD), as shown in Fig. 5, and studied its electrochromic properties. As shown in Fig. 5, applying voltage (an electric field) to the device causes positive ions to transfer toward the electric field. Electrons, on the other hand, go in the reverse direction. The introduction of ions and electrons into the electrochromic (ion storage) layers cause the coloring (bleaching) of the ECDs. The following redox equations can be used to illustrate the underlying physics of electrochromic reactions:



The $rGO@PANI@PB$ thin film changes from colored states to transparent due to electron insertion. However, the electrochromic process that governs the behavior of Li^+ ions in the NiO electrode against ion insertion/extraction may be described by the redox equation (7).



The reduction of Ni^{3+} to Ni^{2+} causes bleaching of the NiO film (throughout the cathodic scan) and coloring of the NiO film via the oxidation of Ni^{2+} to Ni^{3+} (in the opposite process). When a negative voltage is applied continuously to the NiO electrode (ion storage layer), introducing electrons and Li^+ ions, the dominant coloring state develops from the oxidation of Ni^{2+} to Ni^{3+} .

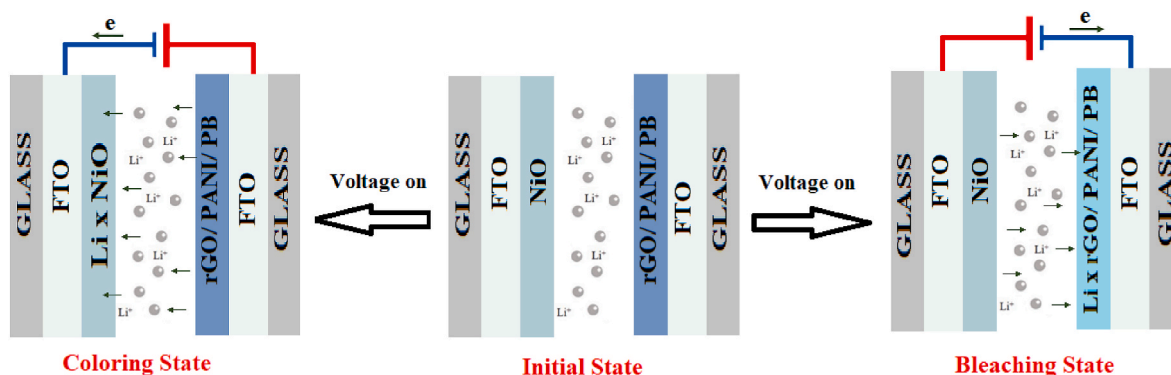


Fig. 5. Schematic diagram for electrochromic device of FTO/NiO/LiClO₄/rGO@PANI@PB

Fig. 6 (a, b) demonstrates the electrochromic performance of ECD (glass/FTO/rGO@PANI@PB/1 M LiClO₄/PC electrolyte/NiO/FTO/glass), which has an active area of $1.4 \times 2.5 \text{ cm}^2$. The in-situ transmittance of $rGO@PANI@PB/NiO$ ECD measured throughout a continuous potential cycle from -0.2 to 1.8 V/SCE is shown in Fig. 6. Fig. 6 (a, b) shows how CA curves and in-situ optical responses of transmittance at a fixed wavelength of 625 nm were used to assess the coloration and bleaching status of ECD. The coloring and bleaching of switching times or speeds distinguished the ECD system. The results show a maximum optical modulation of 41 %, together with the switching durations for coloring (12.1 s) and bleaching (12.6 s) at a wavelength of 625 nm. For 3000 repeated cycles, the ECD showed a high aging value. After the cycles were finished, it was discovered that the ECD transmittance had decreased by 8 %. Table 3 summarizes the electrochromic data for the $rGO@PANI@PB/NiO$ device.

The surface charge capacity ratio of the electrodes in both directions was calculated from the above results of the two materials. According to the following equation, the complementary charge capacity ratio (R) is defined as the extraction NiO electrode charge divided by the intercalation $rGO@PANI@PB$ electrode charge:

$$R = \frac{Q_{out}(NiO)}{Q_{in}(rGO@PANI@PB)} \quad (8)$$

$$Q = \int i dt \quad (9)$$

Q_{in} ($rGO@PANI@PB$) is the surface charge capacity of the $rGO@PANI@PB$ electrode during intercalation, and Q_{out} (NiO) is the surface charge capacity of the NiO electrode during the extraction process. For NiO with an 80 nm thickness and a $rGO@PANI@PB$ layer of 720 nm, the R-value of the ECD was determined to be 78.76 %.

4. Conclusions

Multiple scalable and cost-efficient hybrid films of Prussian blue (PB), rGO , PANI, and NiO have been successfully electrodeposited on FTO glass. Physical characterization of deposited films confirmed that intended properties were achieved on conductive FTO glass. The electrochromic phenomenon of the deposited single, binary, and ternary thin films has been investigated. Moreover, the electrochromic properties were studied for fabricated devices from FTO/rGO@PANI@PB/1 M LiClO₄/PC electrolyte/NiO/FTO/glass. The introduction of rGO was found to cause a decrease in the light transmittance modulation of the composite films due to its light block effect. On the other side, the ternary $rGO/PANI/PB$ nanocomposite films exhibited greater coloring efficiency and quicker switching responses than pure PANI or rGO , due to its larger surface area, particle size, and pore size, as well as the inner interactions between its components. Enhanced cycling stabilities for the composite samples were observed and attributed to rGO presence. In

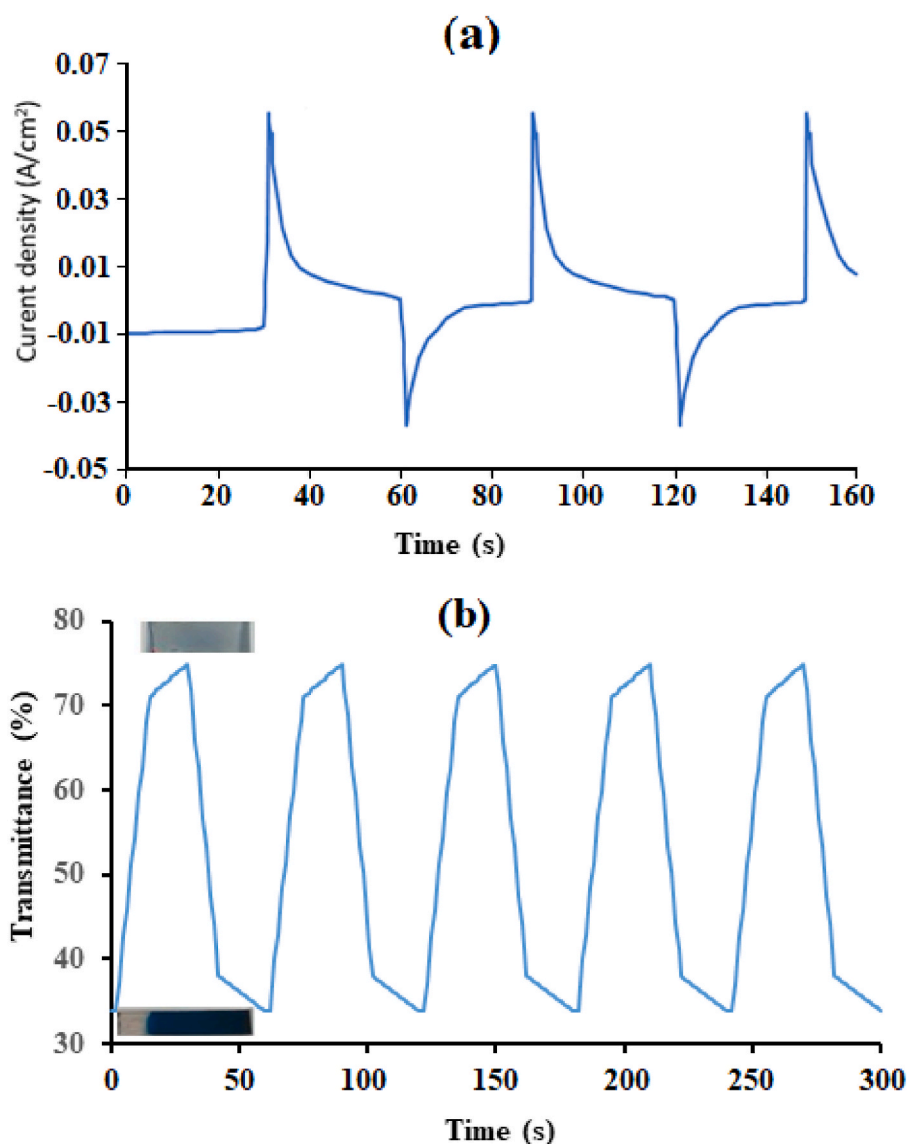


Fig. 6. Electrochromic properties of ECD FTO/PANI@rGO@PB/1 M LiClO₄/P.C. electrolyte/NiO/FTO/glass at wavelength 625 nm and a potential of -0.2 to 1.8 V for 30 s, a) Chronoamperometry curves b) the resulting in-situ visible and solar transmittance.

Table 3

Electrochromic data of FTO/NiO/LiClO₄/PANI@rGO@PB device.

T (λ), nm	Q _{in} Q _{out} mC/cm ²	Reversibility %	Transmittance T _b T _c	Δ.T. %	Color/Bleach time (s) t _c t _b	ΔOD	CE, cm ² /C
625	15.1 12.5	82.8	75 34	41	12.1 12.6	0.34	27.2

summary, the ternary layer rGO/PANI/PB nanocomposite film synergically incorporates the advantages of each of the three individual materials. The ternary-based electrode shows high optical modulation (7.2 % at 600 nm), faster response times ($t_b = 5.7$ s, $t_c = 5.5$ s), and higher CE (11.3 cm²/C). During the durability test, the thickness of the thin film electrode lost 3 % of its original state after 3000 cycles. Moreover, the best performance was achieved for ECD using a ternary material-based electrode (720 nm) in conjunction with 80 nm NiO secondary electrode showing high optical modulation (41 % at 625 nm), fast response times ($t_b = 12.6$ s, $t_c = 12.1$ s) and high CE (27.2 cm²/C) and reversibility of 82.8 %.

CRediT authorship contribution statement

Hala M. Mohamed: Methodology, Software, Data curation, Writing – original draft. **Saad M. Abdel Wahab:** Supervision, Conceptualization, Investigation, Validation, Visualization, Writing – review & editing. **Mohamed M. Abo-Aly:** Supervision, Conceptualization, Investigation, Validation, Visualization, Writing – review & editing. **Mahmoud A. Mousa:** Supervision, Investigation, Conceptualization, Software, Data curation, Validation, Visualization, Writing – original draft, Writing – review & editing. **Asmaa A.I. Ali:** Supervision, Methodology, Data curation, Writing – original draft, Visualization, Investigation, Software, Writing – review & editing.

Declaration of competing interest

The authors declare that they have no known competing financial interests or personal relationships that could have appeared to influence the work reported in this paper.

Data availability

Data will be made available on request.

Acknowledgment

The authors gratefully acknowledge support from the Chemistry Department, Faculty of Science, Benha University, Benha, Egypt, and the Chemistry Department, Faculty of Science, Ain Shams University, Cairo, Egypt.

Appendix A. Supplementary data

Supplementary data to this article can be found online at <https://doi.org/10.1016/j.optmat.2023.114589>.

References

- X. Zhang, M. Zhang, H. Zhang, Z. Jiang, C. Liu, W. Cai, A review on energy, environment and economic assessment in remanufacturing based on life cycle assessment method, *J. Clean. Prod.* 255 (2020), 120160.
- J.A. Palz, D. Campbell-Lendrum, T. Holloway, J.A. Foley, Impact of regional climate change on human health, *Nature* 438 (2005) 310–317.
- H.B. Truelove, C. Parks, Perceptions of behaviors that cause and mitigate global warming and intentions to perform these behaviors, *J. Environ. Psychol.* 32 (2012) 246–259.
- P.V. Rathod, J.M.C. Puguán, H. Kim, Thermo- and electrochromic smart window derived from a viologen-tethered triazolium based poly(NIPAm-TEG-BPV) electrolyte to enhance building energy efficiency and visual comfort, *Chem. Eng. J.* 455 (2023), 140874.
- P.J. Morankar, R.U. Amate, G.T. Chavan, A.M. Teli, D.S. Dalavi, C. Jeon, Improved electrochromic performance of potentiostatically electrodeposited nanogranular WO₃ thin films, *J. Alloys Compd.* 945 (2023), 169363.
- J. Fleury, L. Burnier, M. Lagier, S. Shukla, K. Manwani, E. Panda, A. Schüler, Electrochromic device with hierarchical metal mesh electrodes: transmittance switching in the full spectral range of solar radiation, *Sol. Energy Mater. Sol. Cells* 257 (2023), 112345.
- J.Z. Ou, S. Balendhran, M.R. Field, D.G. McCulloch, A.S. Zoofakar, R.A. Rani, S. Zhuiykov, A.P. O'Mullane, K. Kalantar-Zadeh, The anodized crystalline WO₃ nanoporous network with enhanced electrochromic properties, *Nanoscale* 4 (2012) 5980–5988.
- G.V. Ashok Reddy, K. Naveen Kumar, Ramachandra Naik, V. Revathi, K.M. Girish, K. Munirathnam, Comparative analysis of the effect of post-annealing on CeO₂ and DC Magnetron Sputtered WO₃/CeO₂ nanorods thin films for smart windows, *Applied Surface Science Advances* 16 (2023), 100417.
- X.H. Xia, J.P. Tu, J. Zhang, X.L. Wang, W.K. Zhang, H. Huang, Electrochromic properties of porous NiO thin films prepared by a chemical bath deposition, *Sol. Energy Mater. Sol. Cells* 92 (2008) 628–633.
- M. Gómez, A. Medina, W. Estrada, Improved electrochromic films of NiO_x and WO₃P_y obtained by spray pyrolysis, *Sol. Energy Mater. Sol. Cells* 64 (2000) 297–309.
- Z. Wang, R. Liu, PEDOT:PSS-based electrochromic materials for flexible and stretchable devices, *Mater. Today Electron.* 4 (2023), 100036.
- M.N. Mustafa, M.A.A. Mohd Abdah, A. Numan, A. Moreno-Rangel, A. Radwan, M. Khalid, Smart window technology and its potential for net-zero buildings: a review, *Renew. Sustain. Energy Rev.* 181 (2023), 113355.
- P.M. Beaujuge, J.R. Reynolds, Color control in π -conjugated organic polymers for use in electrochromic device, *Chem. Rev.* 110 (2010) 268–320.
- V.K. Thakur, G. Ding, J. Ma, P.S. Lee, X. Lu, Hybrid materials and polymer electrolytes for electrochromic device applications, *Adv. Mater.* 24 (2012) 4071–4096.
- G.V. Ashok Reddy, K. Naveen Kumar Habibuddin Shaik, Hitha D. Shetty, R. Imran Jafri, Ramachandra Naik, Jyothi Gupta, Sheik Abdul Sattar, B.H. Doreswam, Synthesis, characterizations, and electrochromic studies of WO₃ coated CeO₂ nanorod thin films for smart window applications, *Physica B* 647 (2022), 414395.
- Y. Su, Y. Wang, Z. Lu, M. Tian, F. Wang, M. Wang, X. Diao, X. Zhong, A dual-function device with high coloring efficiency based on a highly stable electrochromic nanocomposite material, *Chem. Eng. J.* 456 (2023), 141075.
- T.E. Olinga, J. Fraysse, J.P. Travers, A. Dufresne, A. Pron, Highly conducting and solution-processable polyaniline obtained via protonation with a new sulfonic acid containing plasticizing functional groups, *Macromolecules* 33 (2000) 2107–2113.
- H. Lyu, J. Liu, S. Mahurin, S. Dai, Z. Guo, X.G. Sun, Polythiophene coated aromatic polyimide enabled ultrafast and sustainable lithium-ion batteries, *J. Mater. Chem. A* 5 (2017) 24083–24092.
- S. Bhadra, D. Khastgir, N.K. Singha, J.H. Lee, Progress in preparation, processing and applications of polyaniline, *Prog. Polym. Sci.* 34 (2009) 783–810.
- W.-f. Liu, Y.-z. Yang, X.-g. Liu, B.-s. Xu, Preparation and electrochemical performance of a polyaniline-carbon microsphere hybrid as a supercapacitor electrode, *N. Carbon Mater.* 31 (6) (2016) 594–599.
- L. Hostert, G.D. Alvarenga, L.F. Marchesi, A.L. Soares, M. Vidottia, One-Pot sono-electrodeposition of poly(pyrrrole)/Prussian blue nanocomposites: effects of the ultrasound amplitude in the electrode interface and electrocatalytic properties, *Electrochim. Acta* 213 (2016) 822–830.
- J. Qian, D. Ma, Z. Xu, D. Li, J. Wang, Electrochromic properties of hydrothermally grown Prussian blue film and device, *Sol. Energy Mater. Sol. Cells* 177 (2018) 9–14.
- Y. Yue, H. Li, K. Li, J. Wang, H. Wang, Q. Zhang, Y. Li, P. Chen, High-performance complementary electrochromic device based on WO₃·0.33H₂O/PEDOT and prussian blue electrodes, *J. Phys. Chem.* 110 (2017) 284–289.
- E. Masetti, F. Varsano, F. Decker, Sputter-deposited cerium vanadium mixed oxide as counter-electrode for electrochromic devices, Sputter-deposited cerium vanadium mixed oxide as counter-electrode for electrochromic devices, *Electrochim. Acta* 44 (1999) 3117–3119.
- M.K. Carpenter, R.S. Conell, D.A. Corrigan, The electrochromic properties of hydrous nickel oxide, *Sol. Energy Mater.* 16 (1987) 333–346.
- C.Y. Tseng, C.W. Hu, K.C. Huang, L.C. Chang, R. Vittal, K.C. Ho, Ion transport across the film of poly (5,6-dimethoxyindole-2-carboxylic acid) in relation to its electrochromic switching: an electrochemical quartz crystal microbalance study, *Electrochim. Acta* 101 (2013) 232–237.
- C.W. Kung, T.C. Wang, J.E. Mondloch, D. Fairen-Jimenez, D.M. Gardner, W. Bury, J.M. Klingsporn, J.C. Barnes, R. Van Duyn, J.F. Stoddart, M.R. Wasielewski, O. K. Farha, J.T. Hupp, Metal-organic framework thin films composed of free-standing acicular nanorods exhibiting reversible electrochromism, *Chem. Mater.* 25 (2013) 5012–5017.
- C.G. Granqvist, *Handbook of Inorganic Electrochromic Materials*, Elsevier, Amsterdam, The Netherlands, 1995.
- P.W. Chen, C.T. Chang, T.F. Ko, S.C. Hsu, K.D. Li, J.Y. Wu, Fast response of complementary electrochromic device based on WO₃/NiO electrodes, *Sci. Rep.* 10 (2020) 8430–8441.
- A. Subrahmanyam, C.C. Kumar, K.M. Karuppasamy, A note on fast protonic solid state electrochromic device: NiO_x/Ta₂O₅/WO₃-x, *Sol. Energy Mater. Sol. Cells* 91 (2007) 62–66.
- H. Li, L. McRae, A.Y. Elezzabi, Solution-processed interfacial PEDOT: PSS assembly into porous tungsten molybdenum oxide nanocomposite films for electrochromic applications, *ACS Appl. Mater. Interfaces* 10 (2018) 10520–10527.
- H.M. Mohamed, M.M. Abo-Aly, S.M. Abdel Wahab, M.A. Mousa, Asmaa A.I. Ali, An electrode for a high-performance asymmetric supercapacitor made of rGO/PANI/PB ternary nanocomposite, *J. Energy Storage* 70 (2023) 108056–108064.
- S.N. Alam, N. Sharma, L. Kumar, Synthesis of Graphene Oxide (G.O.) by Modified Hummers Method and Its Thermal Reduction to Obtain Reduced Graphene Oxide (rGO), *Graphene* 6 (2017) 1–18.
- A. Kumar, A. Kumar, H. Mudila, K. awasthi, V. Kuma, Synthesis and thermal analysis of polyaniline (PANI), *J. Phys.: Conf. Ser.* 1531 (2020), 012108.
- S. Pruneanu, E. Veress, I. Marian, L. Oniciu, Characterization of polyaniline by cyclic voltammetry and UV-Vis absorption spectroscopy, *J. Mater. Sci.* 34 (1999) 2733, 273.
- E. Eren, C. Alver, G.Y. Karaca, E. Uygun, A.U. Oksuz, Enhanced electrochromic performance of WO₃ hybrids using polymer plasma hybridization process, *Synth. Met.* 235 (2018) 115–124.
- E. Eren, G.Y. Karaca, U. Koc, L. Oksuz, A.U. Oksuz, Electrochromic characteristics of radio frequency plasma sputtered WO₃ thin films onto flexible polyethylene terephthalate substrates, *Thin Solid Films* 634 (2017) 40–50.
- Y.E. Firat, A. Peksoz, Efficiency enhancement of electrochromic performance in NiO thin film via Cu doping for energy-saving potential, *Electrochim. Acta* 295 (2019) 645–654.
- R. Giannuzzi, C.T. Prontera, V. Primiceri, A.L. Capodilupo, M. Pugliese, F. Mariano, A. Maggiore, G. Gigli, V. Maiorano, Hybrid electrochromic device with transparent electrolyte, *Sol. Energy Mater. Sol. Cells* 257 (2023), 112346.
- C. Eyvogde, C.S. Deenen, F.R. Zepeda, S. Partling, Y. Smirnov, M.M. Masis, A. S. Arce, H. Grandniers, Color tuning of electrochromic TiO₂ nanofibrous layers loaded with metal and metal oxide nanoparticles for smart colored windows, *ACS Appl. Nano Mater.* 4 (8) (2021) 8600–8610.
- P. Pan, J. Yang, J. Kong, X.J. Loh, J. Wang, Z. Liu, Porous and yet dense[†] electrodes for high-volumetric-performance electrochemical capacitors: principles, advances, and challenges, *Adv. Sci.* 9 (2022) 2103953–2103991, <https://doi.org/10.1002/adv.202103953>.